Journal of Science and Technology, 5(1): 117-132, January 2015

EFFECTS OF HEAT GENERATION AND THERMOPHORESIS ON STEADY MAGNETOHYDRODYNAMIC FREE CONVECTION AND MASS TRANSFER FLOW

M. S. ALAM[1], S. M. CHAPAL HOSSAIN[1] and MOHAMMAD MOKADDES ALI[*2]

[1]Department of Mathematics, Jagannath University, Dhaka-1100, Bangladesh
[2]Department of Mathematics, Mawlana Bhashani Science and Technology University, Tangail-1902, Bangladesh

Abstract

In this paper the effect of thermophoresis on steady magnetohydrodynamic free convective heat and mass transfer flow along an inclined permeable stretching sheet with power-law variation in the surface temperature and concentration in the presence of internal heat generation (or absorption) is studied numerically. The similarity transformations are used to transform the governing equations under consideration into a set of nonlinear coupled ordinary differential equations, which are solved numerically by applying the shooting method together with sixth-order Runge-Kutta integration scheme. The numerical results have been analyzed for the effect of different physical parameters such as magnetic field parameter, suction (or injection) parameter, heat generation (or absorption) parameter, buoyancy parameter, angle of inclination, wall temperature parameter, thermophoresis parameter, and concentration ratio parameter to investigate the flow, heat, and mass transfer characteristics. The results show that higher order temperature and concentration indices has more decreasing effect on the hydrodynamic, thermal and concentration boundary layers compared to the zero order (constant plate temperature and concentration) indices.

Keywords: Heat and mass transfer, inclined stretching sheet, thermophoresis

Introduction

If the temperature gradients across the particle are sufficiently large, thermophoresis causes small particles to move away from the hot wall, and towards the cold one. There are a number of important applications in which thermophoresis phenomenon plays an important role, including plasma flows in which the temperature gradients across the particle are very large. Another would be the erosion process in combustors and heat exchangers in which particles are drawn toward a cool wall in a very hot flow causing fouling or erosion over time. Also, the radiative heat transfer from soot particles can strongly be influenced by thermophoresis because of the large gradients of temperature caused by continuum emission, resulting in particle movement and preferential concentrations, yielding a very complicated coupling between the energy and momentum equations. The fabrication of high yield processors is highly dependant on thermophoresis because of the repulsion and or deposition of impurities on the wafer as it heats up during fabrication. In light of these

[*] Corresponding author: mmali309@gmail.com

various applications, Sasse *et al.* (1994) studied the particle filter based thermophoretic deposition from natural convection flow. Chiou (1998) studied similarity solutions for the problem of a continuously moving surface in a stationary incompressible fluid, including the combined effects of convection, diffusion, wall velocity and thermophoresis for the case in which both the surface temperature and stretching velocity vary as a power-law. Selim *et al.* (2003) analyzed the effect of surface mass transfer on mixed convection flow past a heated vertical flat permeable plate with thermophoresis. Alam *et al.* (2007) studied the effect of variable suction and thermophoresis on steady MHD combined free-forced convective heat and mass transfer flow over a semi-infinite permeable inclined plate in the presence of thermal radiation. Rahman and Postelnicu (2010) investigated effects of thermophoresis on the forced convective laminar flow of a viscous incompressible fluid over a rotating disk. Their results show that if the thermophoretic coefficient increases, thermophoretic velocity increases and it intensifies significantly when the relative temperature difference parameter increases. Very recently, Rahman *et al.* (2012) studied the thermophoresis particle deposition on unsteady two-dimensional forced convective heat and mass transfer flow along a wedge with variable viscosity and variable Prandtl number.

However, in many situations, there may be appreciable temperature difference between the surface and the ambient fluid. This necessitates the consideration of temperature dependent heat source or sinks which may exert strong influence on the heat transfer characteristics. The study of heat generation or absorption effects in moving fluids is important in view of several physical problems such as fluids undergoing exothermic or endothermic chemical reactions. In addition, natural convection with heat generation can be applied to combustion modeling. In view of this importance, Vajravelu and Hadjinicolaou (1997) studied convective heat transfer in an electrically conducting fluid at a stretching surface with uniform free stream in the presence of temperature dependent heat source. Chamkha (1999) studied hydromagnetic three-dimensional free convection on a vertical stretching surface with heat generation or absorption. Abo-Eldahab and El-Aziz (2004) investigated blowing/suction effect on hydromagnetic heat transfer by mixed convection from an inclined continuously stretching surface with internal heat generation/absorption. Chamkha *et al.* (2006) studied the effect of heat generation or absorption on thermophoretic free convection boundary layer from a vertical flat plate embedded in a porous medium.

Billah *et al.* (2011) numerically investigated MHD mixed convection flow and heat transfer characteristics in a double-lid driven cavity with a heat generating solid square block. Rahman *et al.* (2012) studied hydromagnetic slip flow of water based nanofluids past a wedge with convective surface in the presence of heat generation or absorption. Very recently, Rahman and Al-Hadhrami (2013) investigated effects of non-uniform heat sources (or sinks) considering nonlinear slip flow with variable transport properties over a wedge with convective surface.

All of the above studies, however, considered constant wall temperatures and concentrations. But for practical purposes one should also consider a surface having variable wall temperature and concentration. In light of this Chen (2004) studied the combined heat and mass transfer in MHD flow by natural convection from a permeable, inclined surface with variable wall temperature and concentration.

Therefore, the objective of the present work is to investigate the effects of temperature dependent heat generation (or absorption) and thermophoresis on hydromagnetic free convective heat and mass transfer flow of an electrically conducting fluid over an inclined permeable stretching surface with power-law variation in the surface temperature and concentration in the presence of wall suction (or blowing).

Formulation of the Problem and Similarity Analysis

A steady two-dimensional laminar free convective heat and mass transfer flow of a viscous incompressible fluid along a linearly stretching semi-infinite sheet that is inclined from the vertical with an acute angle α is considered. The surface is assumed to be permeable and moving with velocity, $u_w(x) = bx$ (where b is constant called stretching rate). A heat source or sink is placed within the flow to allow for possible heat generation or absorption effects. The fluid is assumed to be Newtonian, electrically conducting and heat generating (or absorbing). The *x*-axis runs along the stretching surface in the direction of motion with the slot as the origin and the *y*-axis is measured normally from the sheet to the fluid. A magnetic field of uniform strength B_0 is applied normal to the sheet in the *y*-direction, which produces magnetic effect in the *x*-direction.

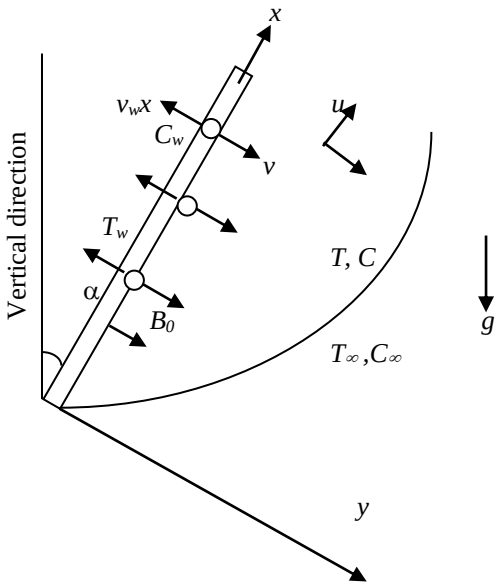

Fig. 1: Flow configuration and coordinate system.

We further assume that (a) due to the boundary layer behavior, the temperature gradient in the y-direction is much larger than that in the x-direction and hence only the thermophoretic velocity component which is normal to the surface is of importance, (b) the fluid has constant kinematic viscosity and thermal diffusivity, and that the Boussinesq approximation may be adopted for steady laminar flow and, (c) the magnetic Reynolds number is small so that the induced magnetic field can be neglected. The configuration and co-ordinate system are shown in Fig. 1.

Under the above assumptions the governing equations describing the conservation of mass, momentum, energy and concentration respectively are as follows:

$$\frac{\partial u}{\partial x}+\frac{\partial v}{\partial y}=0\,, \tag{1}$$

$$u\frac{\partial u}{\partial x}+v\frac{\partial u}{\partial y}=\upsilon\frac{\partial^2 u}{\partial y^2}+g\beta(T-T_\infty)\cos\alpha+g\beta^*(C-C_\infty)\cos\alpha-\frac{\sigma B_0^2}{\rho}u\,, \tag{2}$$

$$u\frac{\partial T}{\partial x}+v\frac{\partial T}{\partial y}=\frac{\lambda}{\rho c_p}\frac{\partial^2 T}{\partial y^2}+\frac{Q_0}{\rho c_p}(T-T_\infty), \tag{3}$$

$$u\frac{\partial C}{\partial x}+v\frac{\partial C}{\partial y}+\frac{\partial(CV_T)}{\partial y}=D\frac{\partial^2 C}{\partial y^2}\,, \tag{4}$$

where the the thermophoretic deposition velocity in the y-direction is given by

$$VT=-\frac{k\upsilon}{T_{ref}}\frac{\partial T}{\partial y} \tag{5}$$

where k is the thermophoretic coefficient and T_{ref} is some reference temperature.

The boundary conditions suggested by the physics of the problem are:

$$u=u_w(x)=bx, v=\pm v_w(x), T_w-T_\infty=A_1x^r, C_w-C_\infty=A_2x^r \text{ at } y=0\,, \tag{6a}$$

$$u=0,\ T=T_\infty,\quad C=C_\infty \text{ as } y\to\infty\,, \tag{6b}$$

where b is a constant called stretching rate and A_1, A_2 are proportionality constants and $v_w(x)$ represents the permeability of the porous surface where its sign indicates suction (< 0) or injection (> 0). Here r is the temperature parameter and for $r = 0$, the thermal boundary conditions become isothermal.

Now, with the help of the similarity variables (Acharya *et al*., 1999):

$$\left.\begin{aligned} &u=\frac{\partial\psi}{\partial y},\ v=-\frac{\partial\psi}{\partial x},\ \psi=(\upsilon b)^{1/2}xf(\eta),\ \eta=(b/\upsilon)^{1/2}y,\\ &\theta(\eta)=(T-T_\infty)/(Tw-T_\infty),\ \varphi(\eta)=(C-C_\infty)/(C_w-C_\infty)\end{aligned}\right\} \tag{7}$$

Equations (2)-(4) become

$$f''' + ff'' - (f')^2 + g_s\theta\cos\alpha + g_c\phi\cos\alpha - Mf' = 0\,, \tag{8}$$

$$\theta'' - r\,Pr\,f\theta + Pr\,f\theta' + Q\,Pr\,\theta = 0, \tag{9}$$

$$\phi'' - rScf\phi + Sc(f + \tau\theta')\phi' + Sc\tau(N_c + \phi)\theta'' = 0\,. \tag{10}$$

The boundary conditions (6) then turn into

$$f = f_w, f' = 1, \theta = 1, \phi = 1 \quad \text{at} \quad \eta = 0\,, \tag{11a}$$

$$f' = 0, \theta = 0, \phi = 0 \qquad \text{as} \quad \eta \to \infty\,, \tag{11b}$$

where $f_w = -v_w/(b\upsilon)^{1/2}$ is the dimensionless wall mass transfer coefficient such that $f_w >$ 0 indicates wall suction and $fw < 0$ indicates wall injection.

The dimensionless parameters introduced in the above equations are defined as: $M = \sigma B_0^2 x/\rho u_w(x)$ is the local magnetic field parameter, $Gr_x = g\beta(T_w - T_\infty)x^3/\upsilon^2$ is the local Grashof number, $Gm_x = g\beta^*(T_w - T_\infty)x^3/\upsilon^2$ is the local modified Grashof number, $\mathrm{Re}_x = u_w(x)x/\upsilon$ is the local Reynolds number, $g_s = Gr_x/\mathrm{Re}_x^2$ is the temperature buoyancy parameter, $g_s = Gm_x/\mathrm{Re}_x^2$ is the mass buoyancy parameter, $Pr = \upsilon\rho c_P/\lambda$ is the Prandtl number, $Q = Q_0 x/\rho c_P u_w(x)$ is the local heat generation/absorption parameter, $Sc = \upsilon/D$ is the Schmidt number, $N_c = C_\infty/(C_w - C_\infty)$ is the dimensionless concentration ratio and $\tau = k(T_w - T_\infty)/T_{ref}$ is the thermophoretic parameter.

The parameters of engineering interest for the present problem are the local skin-friction coefficient, local Nusselt number, and the local Sherwood number which are obtained from the following expressions:

$$Cf_x(\mathrm{Re}_x)^{\frac{1}{2}} = 2f''(0)\,, \tag{12}$$

$$Nu_x(\mathrm{Re}_x)^{-\frac{1}{2}} = -\theta'(0), \tag{13}$$

$$Sh_x(\mathrm{Re}_x)^{-\frac{1}{2}} = -\phi'(0). \tag{14}$$

Results and Discussion

The transformed set of nonlinear ordinary differential equations (8)-(10) together with boundary conditions (11) have been solved numerically by applying Nachtsheim-Swigert (1965) shooting iteration technique [for detailed discussion of the method see Alam *et al.* (2006)] along with sixth order Runge-Kutta integration scheme. A step size of $\Delta\eta = 0.001$ was selected to be satisfactory for a convergence criterion of 10^{-6} in all cases. The results of the numerical computations are displayed graphically in Figs. 2-13 for prescribed surface temperature. Results are obtained for $Pr = 0.70$ (air), $Sc = 0.22$ (hydrogen) and various values of the buoyancy parameters g_s as well as g_c, the magnetic field parameter M, suction (or blowing) parameter f_w, angle of inclination α, surface temperature index r, dimensionless concentration ratio N_c , and thermophoretic parameter τ. The default values of the parameters

are considered as g_s = 12, g_c = 6, *Pr* =0.70, *Sc* = 0.22, $r = 1$, *M* = 0.5, f_w = 0.50, *Q* = 1.0, N_c =1.0, τ = 1.0 and $\alpha = 45^0$ unless otherwise specified.

Figs. 2(a)-(c) represent respectively, the dimensionless velocity, temperature and concentration for various values of the magnetic field parameter (*M*). The presence of a magnetic field normal to the flow in an electrically conducting fluid produces a Lorentz force, which acts against the flow. This resistive force tends to slow down the flow and hence the fluid velocity decreases with the increase of the magnetic field parameter as observed in Fig. 2(a). From Fig. 2(b) we see that the temperature profiles increase with the increase of the magnetic field parameter, which implies that the applied magnetic field tends to heat the fluid, and thus reduces the heat transfer from the wall to the fluid. In Fig. 2(c), the effect of an applied magnetic field is found to increase the concentration profiles, and hence increase the concentration boundary layer thickness.

Figs. 3(a)-(c) depict the influence of the suction (or blowing) parameter f_w on the velocity, temperature and concentration profiles in the boundary layer, respectively. It is known that the imposition of wall suction ($f_w > 0$) has the tendency to reduce all the momentum, thermal as well as concentration boundary layers thicknesses which cause reduction in all the velocity, temperature and concentration profiles. However, the opposite behavior is produced by imposition of the wall fluid blowing or injection ($f_w < 0$) and these behaviors are obvious from Figs. 3(a)-(c).

Representative velocity profiles for three typical angles of inclination (α = 0°, 30° and 60°) are presented in Fig. 4(a). It is revealed from Fig. 4(a) that increased angle of inclination decreases the velocity. The fact is that as the angle of inclination increases the effect of the buoyancy force due to thermal diffusion decrease by a factor of $\cos\alpha$. Consequently, the driving force to the fluid decreases as a result velocity profiles decrease. From Figs. 4(b)-(c) we also observe that both the thermal and concentration boundary layers thicknesses increase as the angle of inclination increases.

The effects of the surface temperature index *r* on the dimensionless velocity, temperature and concentration profiles are displayed in Figs. 5(a)-(c), respectively. From Fig. 5(a) it is seen that, the velocity gradient at the wall increases and hence the momentum boundary layer thickness decreases as *r* increases. Furthermore from Fig. 5(b) we can see that as *r* increases, the thermal boundary layer thickness decreases and the temperature gradient at the wall increases. This means a higher value of the heat transfer rate is associated with higher values of *r*. We also observe from Fig. 5(c) that the concentration boundary layer thickness decreases as the exponent *r* increases.

The effects of heat generation (or absorption) parameter *Q* on the velocity profiles are shown on Fig. 6(a). It is seen from this figure that when the heat is generated ($Q > 0$) the buoyancy force increases, which induces the flow rate to increase giving, rise to the increase in the velocity profiles. Again when the heat absorption ($Q < 0$) intensifies the

velocity is found to decrease due the decrease in the buoyancy force. From Fig. 6(b), we observe that when the value of heat generation parameter ($Q > 0$) increases, the temperature distribution also increases significantly. On the other hand, from Fig. 6(c) we see that the concentration profiles decrease with the increase of heat generation parameter. For heat absorption, an opposite phenomenon is revealed.

The effects of dimensionless concentration ratio (N_c) on the velocity, temperature as well as concentration profiles inside the boundary layer are shown in Figs. 7 (a)-(c), respectively. From these figures we observe that both the momentum and concentration boundary layer thicknesses decrease whereas the thermal boundary layer thickness increases when the values of the concentration ratio (N_c) increases.

The effects of thermophoretic parameter τ on the velocity, temperature as well as concentration distributions are displayed in Figs. 8(a)-(c), respectively. It is observed from these figures that an increase in the thermophoretic parameter τ leads to decrease the velocity across the boundary layer. This is accompanied by a decrease in the concentration and a slight increase in the fluid temperature. This means that the effect of increasing τ is limited **for** increasing the wall slope of the convection profile without any significant effect on the concentration boundary layer.

Figs. 9(a)-(c) show the effects of suction (or blowing) parameter f_w and magnetic field parameter M on the local skin-friction coefficient, local Nusselt number and local Sherwood number, respectively. These figures confirm that as f_w increases, the local skin-friction coefficient decreases whereas both the wall heat transfer and the wall mass transfer increase. But opposite effect is observed for the case of fluid injection or blowing. This phenomenon may be understood from the fact that blowing tends to broaden the concentration distributions, accordingly reduces the wall concentration gradient, and hence the local Sherwood number results.

The effects of surface temperature parameter r and the angle of inclination α, on the local skin-friction coefficient, the local Nusselt number and the local Sherwood number are displayed in Figs. 10(a)-(c), respectively. An increase in the value of r results in a decrease of the local skin-friction coefficient, as shown in Fig. 10(a). Heat transfer results are shown in Fig. 10(b) for some selected values of r. High heat transfer rates can be obtained by increasing the values of r. Moreover, at a given exponent r, the local Nusselt number **decreases** as the angle of inclination α increases. Figure 10(c) presents the effects of r and α on the local Sherwood number. From this figure it is seen that **increased** the value of r enhances the mass transfer rate for all values of α.

In Figs. 11(a)-(c), the effects of Q and g_s on the skin-friction coefficient $Cf_x \operatorname{Re}_x^{1/2}$, the wall heat transfer $Nu_x \operatorname{Re}_x^{-1/2}$ and the wall mass transfer $Sh_x \operatorname{Re}_x^{-1/2}$ are presented, respectively. From these figure we see that for a fixed value of g_s, both the local skin-friction coefficient and the local Sherwood number increases whereas the local Nusselt number decreases with the increasing values of the heat generation parameter ($Q > 0$).

But opposite effects are observed for the case of heat absorption ($Q < 0$). Free convection effect is also clear from these figures.

The effects of the dimensionless concentration ratio N_c and the mass buoyancy parameter g_c on the local skin-friction coefficient, the local Nusselt number and the local Sherwood number are shown in Figs. 12 (a)-(c), respectively. From these figures we see that for all values of g_c, both the local skin-friction coefficient and local Nusselt number decreases whereas the local Sherwood number increases when the values of N_c increase. From Fig. 12(a) we also observe that for a fixed N_c, the increase in the buoyancy force leads to an increase in the drag coefficient.

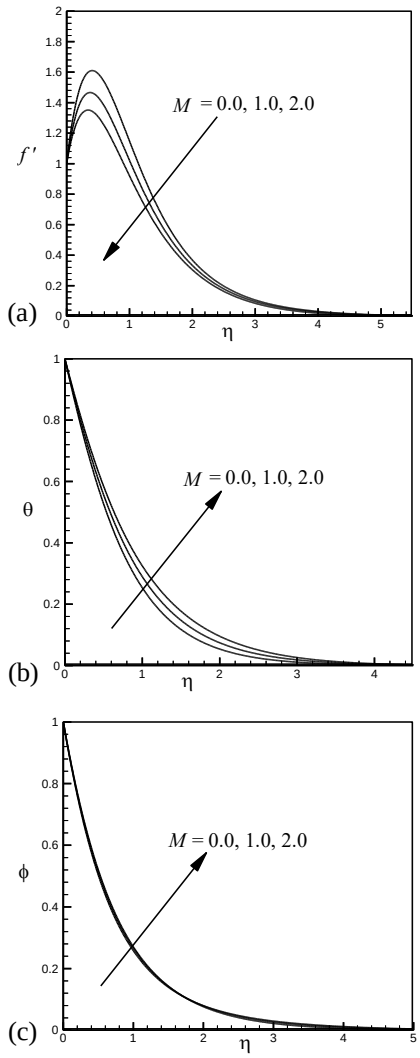

Fig. 2. Dimensionless (a) velocity, (b) temperature and (c) concentration profiles for different values of M

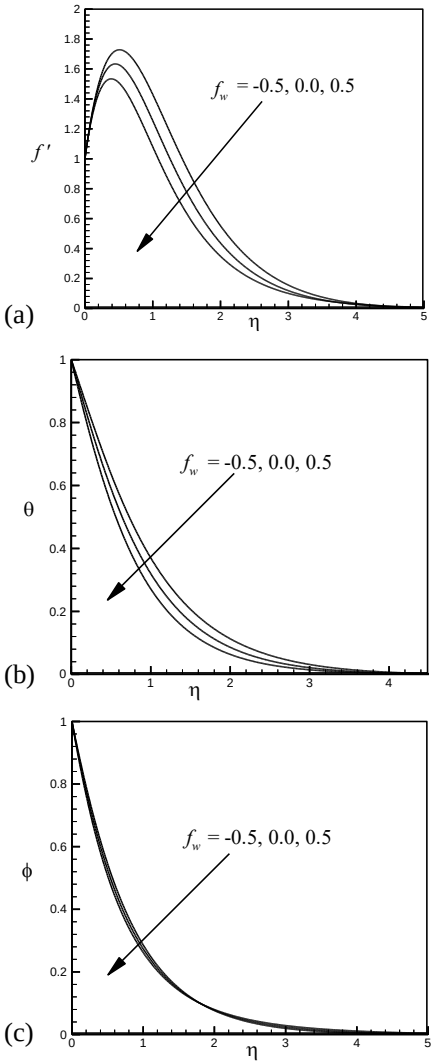

Fig. 3. Dimensionless (a) velocity, (b) temperature and (c) concentration profiles for different values of f_w

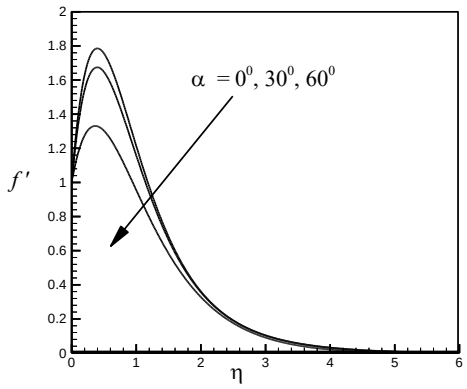

(a)

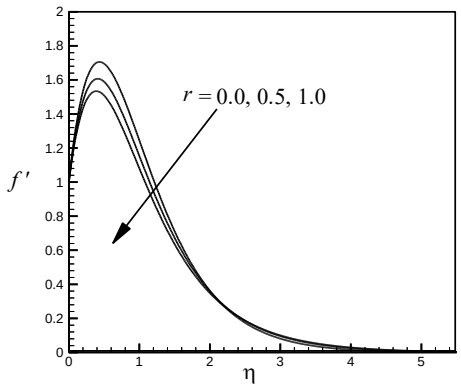

(b)

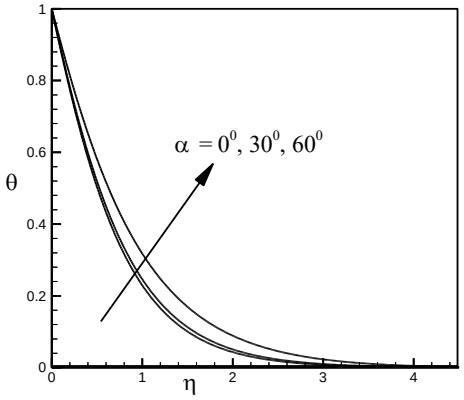

(a)

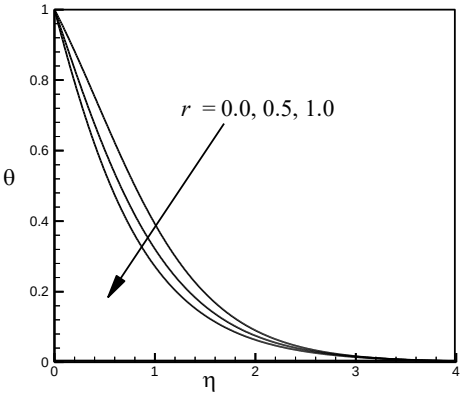

(b)

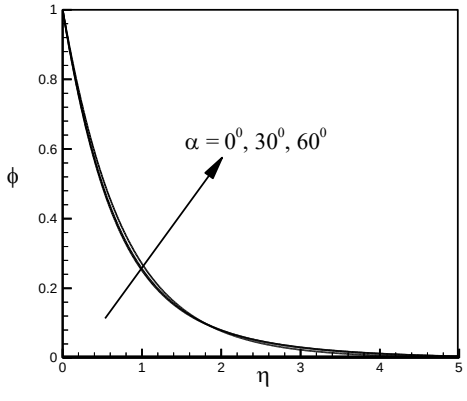

(a)

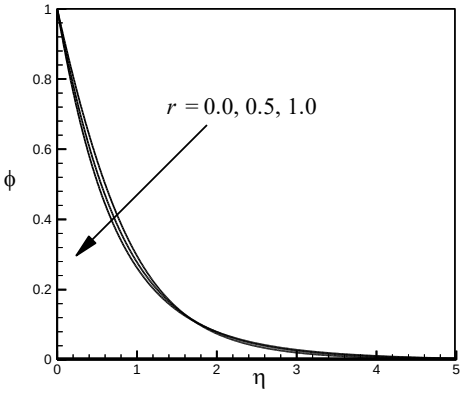

(b)

Fig. 4. Dimensionless (a) velocity, (b) temperature and (c) concentration profiles for different values of α.

Fig. 5. Dimensionless (a) velocity, (b) temperature and (c) concentration profiles for different values of r.

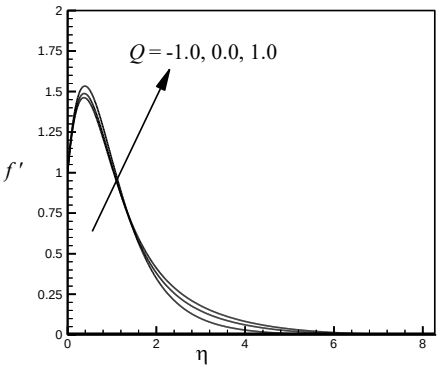

(a)

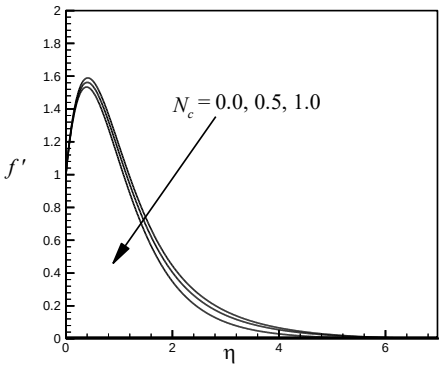

(b)

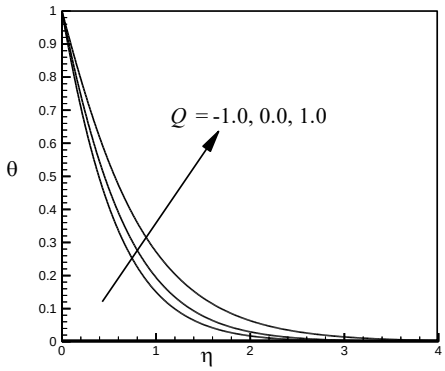

(a)

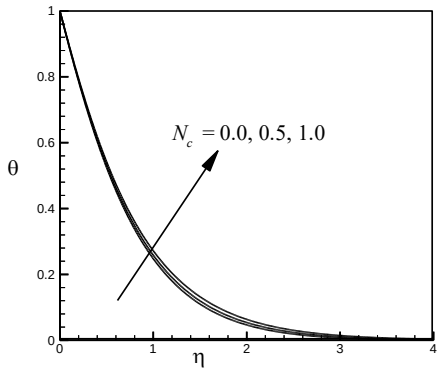

(b)

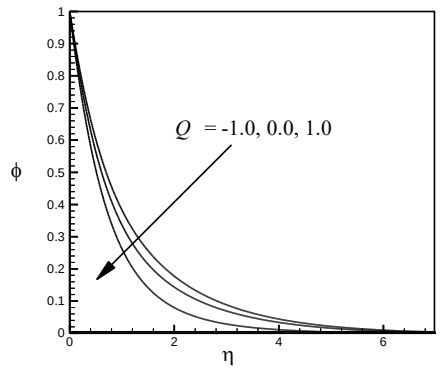

(a)

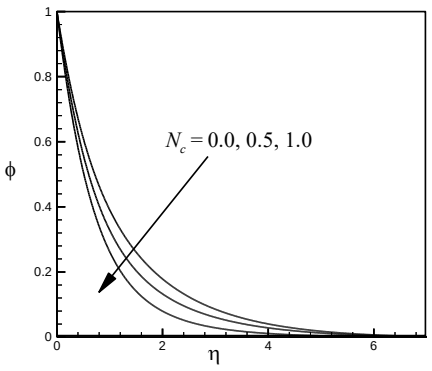

(b)

Fig. 6. Dimensionless (a) velocity, (b) temperature and (c) concentration profiles for different values of *Q*.

Fig. 7. Dimensionless (a) velocity, (b) temperature and (c) concentration profiles for different values of N_c.

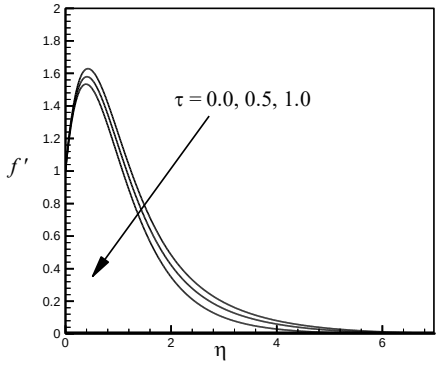

(a)

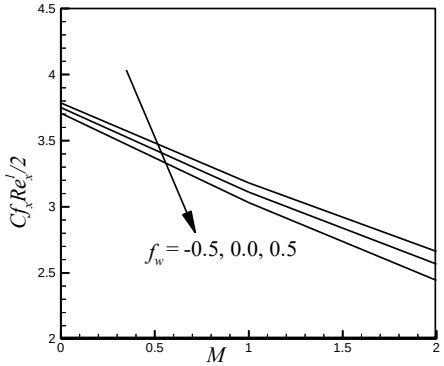

(b)

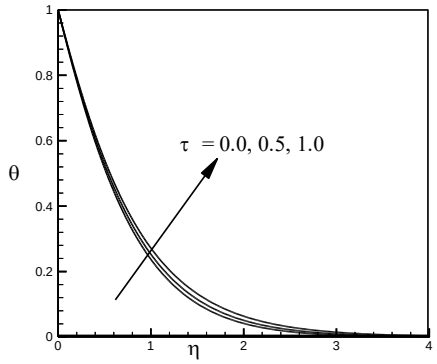

(a)

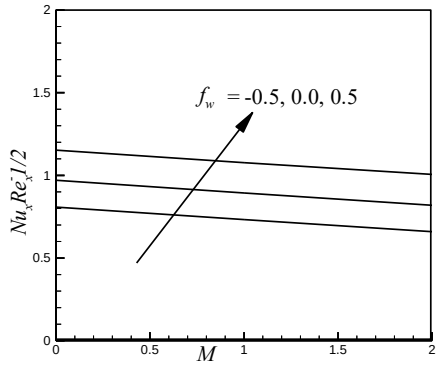

(b)

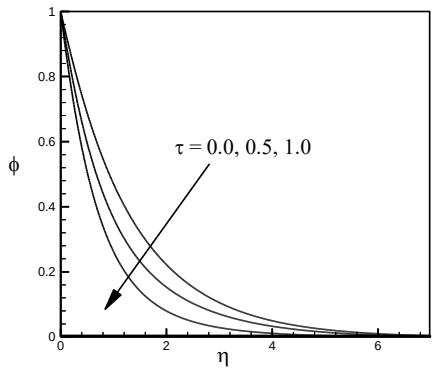

(a)

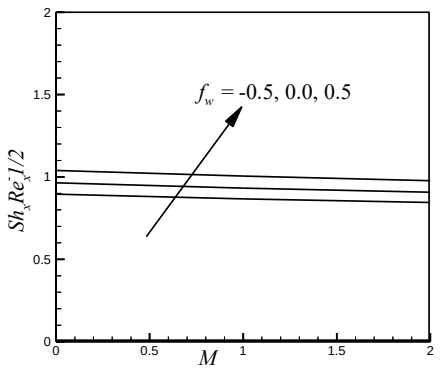

(b)

Fig. 8. Dimensionless (a) velocity, (b) temperature and (c) concentration profiles for different values of τ..

Fig. 9. Effects of f_w and M on (a) local skin-friction coefficient, (b) local Nusselt number, and (c) local Sherwood number respectively.

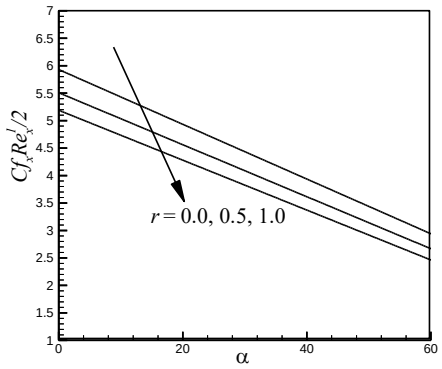

(a)

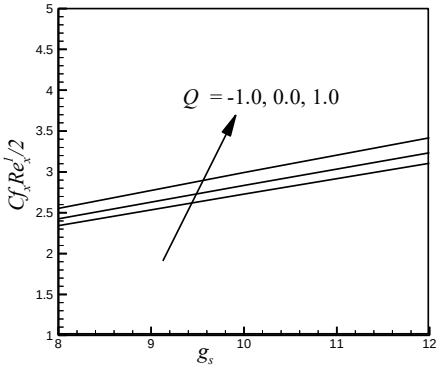

(b)

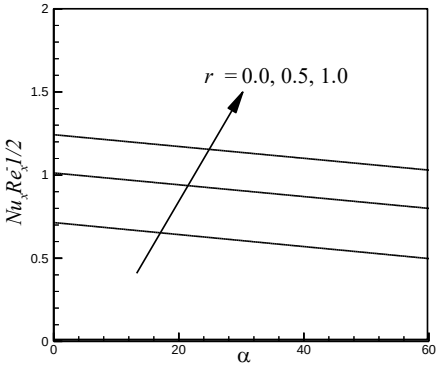

(a)

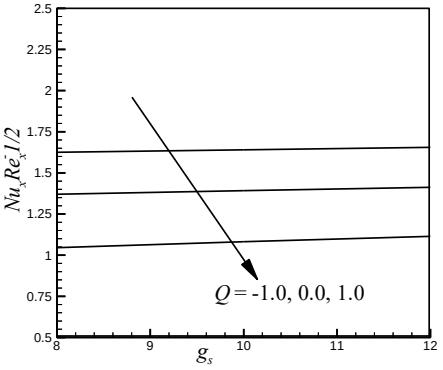

(b)

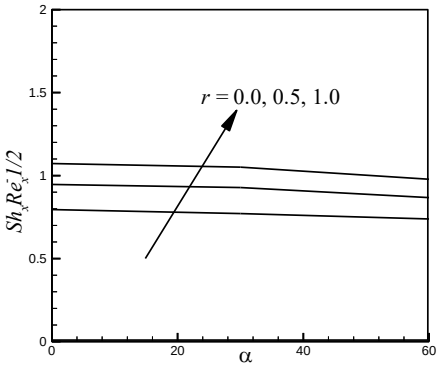

(a)

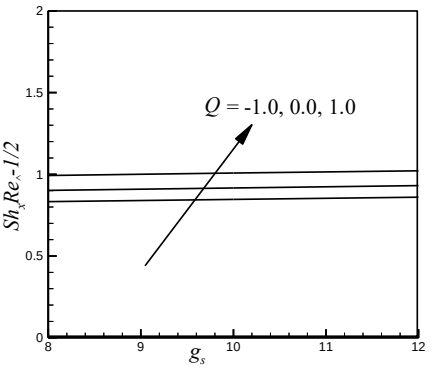

(b)

Fig. 10. Effects of r and α on (a) local skin-friction coefficient, (b) local Nusselt number, and (c) local Sherwood number respectively.

Fig. 11. Effects of Q and g_s on (a) local skin-friction coefficient, (b) local Nusselt number, and (c) local Sherwood number respectively.

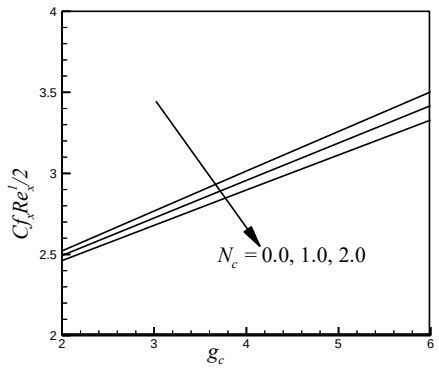

(a)

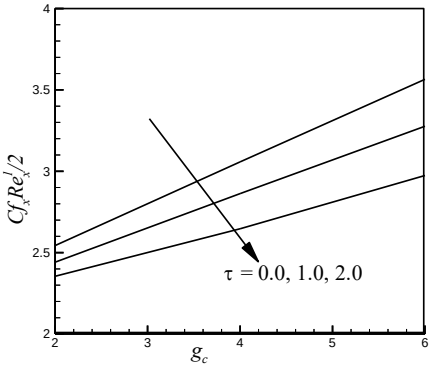

(b)

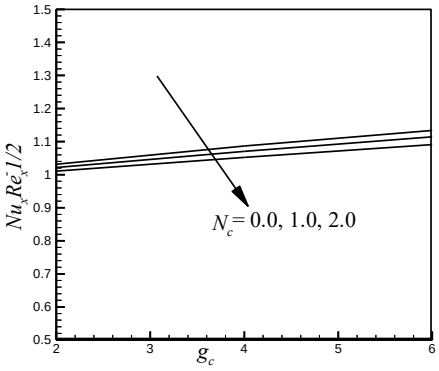

(a)

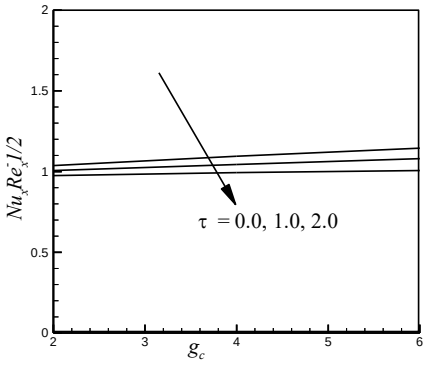

(b)

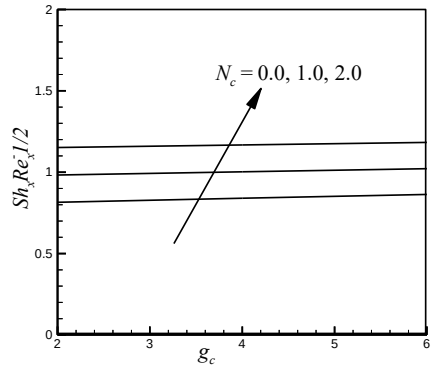

(a)

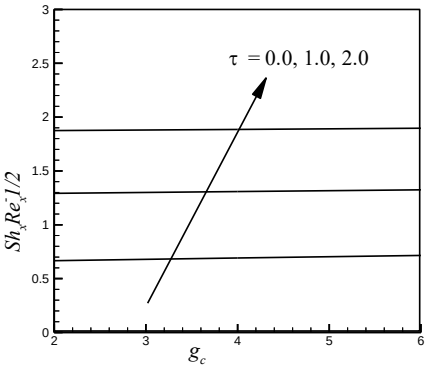

(b)

Fig. 12. Effects of N_c and g_c on (a) local skin-friction coefficient, (b) local Nusselt number, and (c) local Sherwood number respectively.

Fig. 13. Effects of τ and g_c on (a) local skin-friction coefficient, (b) local Nusselt number, and (c) local Sherwood number respectively.

The effects of the thermophoretic parameter τ and the mass buoyancy parameter g_c on the local skin-friction coefficient, the local Nusselt number and the local Sherwood number are shown in Figs. 13 (a)-(c), respectively. From these figures we see that the local skin-friction coefficient as well as local Nusselt number decreases whereas the local Sherwood number increases with an increasing values of the thermophoretic parameter for all values of g_c.

Conclusion

In this paper the effects of heat generation (or absorption) and thermophoresis on hydromagnetic buoyancy-induced natural convection flow of a viscous, incompressible, electrically-conducting fluid along an inclined permeable surface with variable wall temperature and concentration has been investigated numerically. The governing equations are developed and transformed using appropriate similarity transformations. The transformed similarity equations are then solved numerically by applying shooting method. From the present numerical investigations the following conclusions may be drawn: i) The fluid velocity inside the boundary layer decreases with the increasing values of the magnetic field parameter, suction parameter, angle of inclination, concentration ratio as well as thermophoretic parameter whereas it increases with increasing values of the heat generation parameter. ii) The temperature distribution increases with the increasing values of the magnetic field parameter, angle of inclination, heat generation parameter, and concentration ratio as well as thermophoretic parameter whereas it decreases with an increasing value of the suction parameter. iii) The concentration profile increases with an increasing value of the magnetic field parameter and angle of inclination whereas it decreases with the increasing values of the suction parameter, heat generation parameter, concentration ratio as well as thermophoretic parameter. iv) Higher order temperature and concentration indices has more decreasing effect on the hydrodynamic, thermal and concentration boundary layers compared to the zero order (constant plate temperature and concentration) index. v) The local skin-friction coefficient decreases with the increasing values of the magnetic field parameter, suction parameter, angle of inclination to the vertical, power-law exponent, concentration ration as well as thermophoretic parameter whereas it increases with an increasing values of heat generation parameter. vi) The local Nusselt number decreases with an increasing values of the angle of inclination, heat generation parameter, concentration ratio and thermophoretic parameter whereas it increases with the increasing values of the wall temperature and concentration exponent as well as suction parameter. vii) The local Sherwood number increases with an increasing values of suction parameter, the power-law exponent, concentration ratio, heat generation parameter and thermophoretic parameter whereas it decreases with the increasing values of the angle of inclination.

References

Abo-Eldahab, E.M. and M.A. El-Aziz, (2004). Blowing/suction effect on hydromagnetic heat transfer by mixed convection from an inclined continuously stretching surface with internal heat generation/absorption. *Int. J. Thermal Sciences*, **43:** 709-719.

Acharya, M., L.P. Singh and G.C. Dash G.C., (1999). Heat and mass transfer over an accelerating surface with heat source in the presence of suction and blowing. *Int. J. Engng. Sci*., **37:** 189-211.

Alam, M.S., M.M. Rahman and M.A. Sattar, (2008). Effect of variable suction and thermophoresis on steady MHD combined free-forced convective heat and mass transfer flow over a semi-infinite permeable inclined plate in the presence of thermal radiation. *Int. J. Thermal Sciences*, **47:** 758-765.

Alam, M.S., M.M. Rahman and M.A. Samad, (2006). Numerical study of the combined free-forced convection and mass transfer flow past a vertical porous plate in a porous medium with heat generation and thermal diffusion, Non-linear Analysis: Modeling and Control, **11:** 331-343.

Alam, M.S. and M.M. Rahman, (2013). Effects of variable wall temperature and concentration on heat and mass transfer of MHD natural convection flow past an inclined surface with thermophoresis. *International Journal of Energy & Technology*, **5:** 1-11.

Alam, M.S. and M.M. Rahman, (2014). Thermophoretic deposition effect on transient free convection hydrodynamic flow along an accelerated inclined permeable surface with time dependent temperature and concentration. *Heat transfer-Asian Research*, **43(4):** 352-367.

Billah, M.M., M.M. Rahman, R. Saidur and M. Hasanuzzaman, (2011). Simulation of MHD mixed convection heat transfer enhancement in a double lid-driven obstructed enclosure. *Int. J. Mechanical and Materials Engineering*, **6(1):** 18-30.

Chamkha, A.J., (1999). Hydromagnetic three-dimensional free convection on a vertical stretching surface with heat generation or absorption. *Int. J. Heat Fluid Flow*, **20:** 84-92.

Chamkha, A.J., A.F. Al-Mudhaf and I. Pop, (2006). Effect of heat generation or absorption on thermophoretic free convection boundary layer from a vertical flat plate embedded in a porous medium. *Int. Commun. Heat and Mass Transfer*, **33(9):** 1096-1102.

Chen, C.H., (2004). Heat and mass transfer in MHD flow by natural convection from a permeable inclined surface with variable wall temperature and concentration. *Acta Mechanica*, **172:** 219-235.

Chiou, M. C., (1998). Effect of thermophoresis on submicron particle deposition from a forced laminar boundary layer flow onto an isothermal moving plate. *Acta Mechanica*, **129:** 219-229.

Nachtsheim, P.R. and P.Swigert, (1965). Satisfaction of the asymptotic boundary conditions in numerical solution of the system of non-linear equations of boundary layer type, NASA TND-3004.

Rahman, M.M. and A.Postelnicu, (2010). Effects of thermophoresis on the forced convective laminar flow of a viscous incompressible fluid over a rotating disk. *Mech. Res. Commun*, **37:** 598-603.

Rahman, ATM. M., M.S. Alam and M.K. Chowdhury, (2012). Thermophoresis particle deposition on unsteady two-dimensional forced convective heat and mass transfer flow along a wedge with variable viscosity and variable Prandtl number. *Int. Communications in Heat and Mass Transfer*, **39:** 541-550.

Rahman, M.M., M.A. Al-Lawatia, I.A. Eltayeb and N. Al-Salti, (2012). Hydromagnetic slip flow of water based nanofluids past a wedge with convective surface in the presence of heat generation (or) absorption. *Int. J. Thermal Sciences*, **57:** 172-182.

Rahman, M.M. and A.M.K. Al-Hadhrami, (2013). Nonlinear slip flow with variable transport properties over a wedge with convective surface, Proceedings of the 4th Interdisciplinary Chaos Symposium on Chaos and Complex Systems, 167-181.

Sasse, A.G.B.M., W.W. Nazaroff and A.J. Gadgil, (1994). Particle filter based thermophoretic deposition from natural convection flow, *Aerosol Science and Technology*, **20(3):** 227-238.

Selim, A., M.A. Hossain and D.A.S. Rees, (2003). The effect of surface mass transfer on mixed convection flow past a heated vertical flat permeable plate with thermophoresis. *Int. J. Thermal Sciences*, **42:** 973-982.

Vajravelu, K. and A. Hadjinicolaou, (1997). Convective heat transfer in an electrically conducting fluid at a stretching surface with uniform free stream. *Int. J. Engng. Sci.*, **35:** 1237-1244.